
Fiber Tapering and Dimpling for Evanescent Coupling

Author:
Gregory van Beek

June 5, 2015

Fiber Tapering and Dimpling for Evanescent Coupling

Gregory van Beek

to obtain the degree of Bachelor of Engineering
at the Hague University Delft,
to be defended on Wednesday June 24, 2015 at 10.00 AM.

The Hague University of Technology, Innovation and Society Delft
Department of Applied Physics
Student number: 11086882

Delft University of Technology
Faculty of Applied Sciences
Department of Quantum Nano Science.
Project duration: February 9, 2015 - June 5, 2015

First Coach : Dr. A.J. Lock HHS
Second Coach : Dr. R.A. Mantel HHS
Supervisor : Dr. S. Gröblacher TUD

Thesis Committee : Dr. A.J. Lock
Dr. R.A. Mantel
Ir. J. Zelisse

THE HAGUE
UNIVERSITY
OF APPLIED SCIENCES

 **TU Delft** Delft
University of
Technology

Acknowledgments

Despite a relative short internship of about five months for my bachelor thesis, I wanted to write a short acknowledgment for the people that helped me during this period. First, of course, I want thank Simon for your patience and the explanations you gave about even the simplest things like properly connecting a fiber into a laser. But also for the support for some of my ideas and out designs like an early setup that was resting on just a pair tissue boxes. I also want to give thanks to Alex for the tips you gave in the beginning and to João who helped me numerous of times in the lab for searching for things and explaining about his setup what was actually really informative for me. Also thanks to the rest of the team, Teo, Richard and Luka for helping me having a great time during my internship. And of course Igor, despite I have worked with for two small weeks, who gave me some tips and critics about the way I was calculating things and approaching problems with the fibers. And I definitely cannot forget to mention Tino for turning my ideas into proper drawings and making them exactly as I wanted it and because of the warning about the homemade illegal power plugs that João and I where fabricating.

Finally I want to thank my parents and my girlfriend for having a lot of patience with me and supporting me when I had some hard times getting this thesis ready on time and, Ivana, sorry for missing some of our dance lessons because I planned things badly.

*Gregory van Beek
Delft, June 5, 2015*

Abstract

For evanescent coupling of optical fibers with small optical devices, a tapered fiber can be used. A small region of the fiber is thinned out to increase the evanescent field of the guided light wave. The process of tapering a fiber (a CORNING SMF-28e+) begins with heating the fiber with a hydrogen flame. This allows the fiber to get softer and when it is getting pulled, the diameter of the heated part of the fiber (the hot-zone) shall decrease because of the conservation of mass. This pulling is accomplished with pulling stages where both ends of the fiber are clamped on. These stages move synchronized, so that the fiber is equally stretched from both sides creating two equal transition regions. The fiber starts as a single mode fiber at the used wavelength of $\lambda = 1550\text{nm}$. During heating, the core and the cladding melt together creating one relatively large fiber with the surrounding air as cladding. This causes the fiber to become multimode. As it is pulled, the transmission output shows oscillations because of the constantly changing interference of the different light paths. When these oscillations stop, there will be no interference anymore indicating that the fiber is single mode again. The measurements are done with several pulling speeds in the range $30\mu\text{m s}^{-1} < v < 50\mu\text{m s}^{-1}$. The highest transmissions are found at a pulling distance around 12mm and higher with an average of 85%. A large pulling length gives a gradually decay of the transition region towards the thin part of the fiber. If this transition region is too small, the light can get easier refracted, resulting in (bigger) losses. The diameter of the fiber where it becomes single mode is calculated to be around $1,2 \pm 0,30\mu\text{m}$. After several measurements, the diameter of the tapered region of the fiber is on average around $2\mu\text{m}$ to $2,5\mu\text{m}$. The difference between the calculated and the measured value can be occurring because the pulling is probably not always stopped exactly when the fiber is becoming single mode. At some measurements, the point where the oscillations stop is not always clear to see due to fluctuations in the transmission that are present during pulling because of, for example, misalignment. This means it can happen that some pullings are stopped when the fiber is still multi mode and it should have been pulled for a little longer. If this is pulled for longer, the diameter of the tapered region can come close to the expected value. Some fibers are pulled to a diameter of $1,5\mu\text{m}$ without breaking or gaining severe losses. This is within the error of the calculated diameter. The transmission efficiencies can go up to 90% to 98% if the setup is properly aligned and the fibers are prepared well. The position of the hydrogen torch relative to the fiber is an important quantity that can influence the measurement, because a large part of the fiber needs to be within the flame to create a large tapered region. This proved to be the most important factor and this should be positioned with care.

Contents

1	Introduction	1
1.1	General uses of photonic integrated circuits	1
1.2	Scope of the research	2
1.3	Thesis outline	3
2	Transmission in optical fibers	4
2.1	Propagation of light	4
2.2	Evanescent wave	7
2.3	Tapering a fiber	11
2.4	Heating a fiber	13
2.5	Dimpling a fiber	14
3	Experimental Set-Up	15
3.1	Preparations for tapering	17
3.2	Preparations for dimpling	19
3.3	Validation	20
4	Transmission measurements	23
4.1	Transmission efficiency during pulling	23
4.2	Tapering diameter	27
4.3	Error analysis	30
5	Conclusion	32
	References	34
A	Supplementary information chapter 3	36
B	Tables	38

1 Introduction

1.1 General uses of photonic integrated circuits

Most electronic devices are fitted with integrated circuits (IC). Those circuits are commonly fabricated with the use of photolithography, which can print electronic components on a scale of tens of nanometres. Because these IC components can be made on a very small-scale, a single chip can contain a large quantity of components (e.g. transistors). This makes it relatively cheap to produce. The number of tasks a single integrated circuit can do, is for a part depending of the number of transistors it contains. In order to make a chip that can handle a great number of tasks at the same time means the number of transistors need to increase. This is the basis of Moore's law, which states that the number of transistors will double every two years to keep up with the increasing demand of speed a single computer needs to reach. This has turned out to be a good approximation over the last decades. But there will eventually be a point that these IC's simply can't contain even more components without increasing the size [1].

One of the alternatives of electronic circuits are photonic integrated circuits (PIC). These are a circuits based on the input and output of light instead of electrons, usually around the visible and near-infrared frequencies. Photonic integrated circuits are commonly used in optical fiber communications. The main advantages of PIC in comparison with electronic ICs are the speed and bandwidth. PIC's uses the different wavelengths of the light to carry information with the speed of light. Besides are PIC's immune to electromagnetic radiation, which in some applications can be favored.

One of the reasons that PIC's are not widely used has to do with a couple of disadvantages PIC's have. A lot of research, for example, is currently going into making the optical devices smaller. Light needs to be transported by waveguides, which cannot be a lot smaller than the wavelength that is guided. Besides are sharp bends not easy to fabricate while keeping a low optical loss. Also optical connections are harder to produce while preventing lots of losses in comparison with those of electronic based circuits [3] [4].

1.2 Scope of the research

One of the components that a photonic integrated circuit may contain is an optical resonator. A common resonator is for example a laser cavity, which guides the light through a gain medium to amplify the light. Those cavities can also be used as a time delay of the light. When a ray is guided in an optical cavity, the path length increases. The ray therefore needs more time to cover a path that includes an optical cavity in comparison with the same path but without a cavity.

An optical cavity can also be made as a ring. This is the so-called ring resonator, which is one of the possibilities of filtering a desired wavelength. Only specific wavelengths will be allowed in the resonator due to interference of light after it is guided for a full cycle. This is mainly depending on the size of the resonator and the quality of the cavity. The tolerances in the size of these resonators are small (order of magnitude of about the used wavelength) because a small inaccuracy will result in a wrong wavelength filter or (a lot) of optical losses.

To check the size and quality of an optical ring resonator, several known wavelengths will be coupled in. Depending on which wavelength is passed through the resonator the size can be calculated because the path length of the light within the resonator must be a multiple of the wavelength for constructive interference. So, for light to be able to pass through the resonator it must obey

$$l_{resonator} = 2\pi m \cdot \lambda$$

where $l_{resonator}$ is the path length light covers in the resonator, λ is the wavelength of the guided light and m is an integer.

Light can be coupled in a ring resonator by using an evanescent field from a glass fiber. To make this as efficient as possible, the refractive indices of the initially guiding fiber and the cavity (or any other optical waveguide) needs to be matched and the fiber that guides the light needs to be as thin as possible. Narrowing, or tapering, the fiber can be achieved by heating a small part of the fiber followed by stretching it from both sides. During the heating and pulling the fiber becomes longer and smaller. The field of the lightwave outside the fiber shall increase and so the field can be transported to, for example, a cavity or a waveguide. This will be further explained in this thesis.

For better control of this coupling of light to another waveguide, a small dimple can be made in the fiber. Only the part of the fiber with this dimple is brought close enough to the device and only there the coupling will take place.

This thesis describes a method that can be used to taper and dimple a fiber. The main focus of the research is on getting tapered fibers where the thinner part provides low to no optical losses. Other research groups (like [6] and [7]) claimed to have tapered fibers with less than 1% loss of optical signal. The diameter of the fiber, which is a basic fiber used for optical communications with a initial diameter of 125 μm , can get around 1 μm after tapering. This experiment will be reproduced to make our own tapered fibers for optical coupling into other devices while maintaining low optical losses (i.e. $\leq 5\%$ optical losses). Herefore a setup will be build and tested on efficiency and reproducibility. Also a setup will be described for dimpling the fiber. This dimpling setup should be able to produce a little peak (i.e. a dimple of a couple of microns) in the fiber while keeping additional losses to under a few per cent relative to the transmission after tapering.

1.3 Thesis outline

In this thesis the setup of tapering and dimpling a fiber will be discussed. The second chapter will cover the theoretical aspect of the project and the theory about the tapering and the dimpling. The third chapter describes the setup that is used to pull the fibers and for the dimpling and describes the validation of the setup. In the fourth chapter are the measurements and the results discussed. This also includes a error analysis of the results. In appendix A is some supplementary information added about the equation used in chapter three. There is a list of the measurements that has been done attached in appendix B. As last the original description of the project is attached.

2 Transmission in optical fibers

A typical component of a photonic integrated circuit is a ring resonator. The theory of a ring resonator is based on a theory of whispering gallery modes.

This acoustic phenomenon was discovered by lord Rayleigh in the late nineteenth century in the dome of the St Pauls Cathedral in London. When someone is sitting near the wall, that persons whisper can be heard on specific locations in the dome around a distance for several metres. A sound wave coming from the whisper can travel around the dome repeatedly reflecting of the wall [2].

Light in a ring resonator can have the same effect, based on destructive- and constructive interference. This means that only specific wavelengths that constructively interfere will be guided in the resonator [5].

2.1 Propagation of light

The coupling of the light with the optical resonator (or any other optical device) can be achieved with the use of an evanescent wave that exist outside the fiber.

The fiber initially exist as a core with a refractive index n_1 and a cladding with refractive index n_2 . For total internal reflection (TIR) to occur in the fiber, the angle of incidence should obey Snell's law. This states that the maximum angle of incidence is

$$\sin(\theta_c) = \frac{n_2}{n_1} \quad (2.1)$$

where θ_c is the critical angle [rad], which is the maximum angle that light can make so that TIR can occur.

Because the left part of the equation cannot exceed one, the ratio between n_1 and n_2 should obey

$$n_1 > n_2$$

The maximum angle of which the light can be coupled in can be derived with substituting equation (2.1) in Snell's law. This follows

$$\sin(\theta_{i,max}) = \frac{1}{n_o} \sqrt{(n_1^2 - n_2^2)} \quad (2.2)$$

where n_o is the refractive index of the incidence medium and $\theta_{i,max}$ [rad] is the maximum angle of incidence with respect to the centre of the fiber (See figure 2.1) [18].

This maximum angle of incidence is typically expressed in the numerical aperture (NA), which is defined as

$$\begin{aligned} NA &= n_0 \cdot \sin(\theta_{i,max}) \\ &= \sqrt{n_1^2 - n_2^2} \end{aligned} \quad (2.3)$$

This equations shows that the NA will be in the range $0 < NA < 1$ if the incident ray of light is traveling in air. If the NA is for example equal to one, than the $\sin(\theta_{i,max})$ from equation (2.2) will have also have to be one, which is at an angle of 90 degrees. This means that all the angles in a range between 0 and 90 degrees will undergo TIR. So, the higher the NA is, the greater the maximum angle is and the easier it is to couple light in the fiber. For multimode fibers the NA can be anywhere between 0,3 to close to 1,0 depending on the refractive indices of the core and the cladding [10].

For single mode fibers the NA is typically small, around 0,1. This means that when the incidence medium is air ($n_0 \approx 1,0$) the maximum $\theta_{i,max}$ is about 5,7 degrees.

It can be important, as we will see, to relate the wavelength λ of the light in the fiber to the fiber properties. This is done in the so-called V-number, or normalized frequency. This V-number is defined as

$$\begin{aligned} V &= \frac{\pi 2a}{\lambda} \sqrt{n_1^2 - n_2^2} \\ &= \frac{\pi 2a}{\lambda} \cdot NA \end{aligned} \quad (2.4)$$

When $V \leq 2,4048$, the fiber is said to be single mode. At a given wavelength the diameter ($d = 2a$) of the fiber where it becomes single mode can be determined [12] [6].

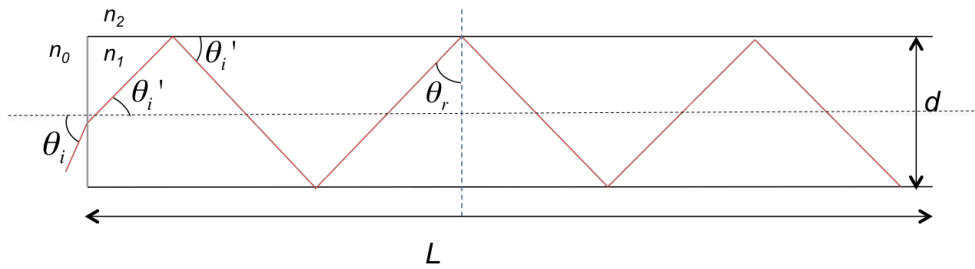


Figure 2.1: Ray of light in an optical fiber. Shown are, respectively, the angles of incidence outside (θ_i) and inside (θ_i') the fiber and the angle of reflection (θ_r). L is the total length of the fiber, d is the diameter and n_1 and n_2 are the refractive indices of the core and the cladding respectively.

The number of different modes M that are allowed in the fiber can be estimated with the V-parameter

$$M \approx \frac{V^2}{2} \quad (2.5)$$

One has to keep in mind that if the diameter of the fiber is in the same order as the wavelength, the wave nature of light cannot be ignored anymore.

The given equations do give a good estimation of the parameters though and will therefore be used.

The light rays can thus follow multiple routes in the fiber. This means, because the speed of light c is constant in a specific medium, the time it takes to reach the end of the fiber differs for the different routes. Higher modes have longer paths (more reflections) and therefore need more time to reach the end of the fiber. This is better known as intermodal dispersion. (See figure 2.2) [19].

But the higher modes usually penetrate more in the cladding than the lower modes (the evanescent field, see paragraph 2.2).

The core of the fiber has a higher refractive index than the cladding of the fiber, which means that the group velocity of light in the cladding is higher than in the core.

So a higher mode travels a greater distance, but because the mode is more in the cladding than a lower mode, the speed is higher. This changes the definition of the intermodal dispersion, because the time difference is not only depending on the difference of the several routes, but also on the change in velocity between the core and the cladding.

The general definition of the velocity of light in a medium is given by the ratio between the speed of light in vacuum and the refractive index of that medium. For the group velocity of light, the wavelength becomes important because the refractive index of a medium is depending on the propagating wavelength.

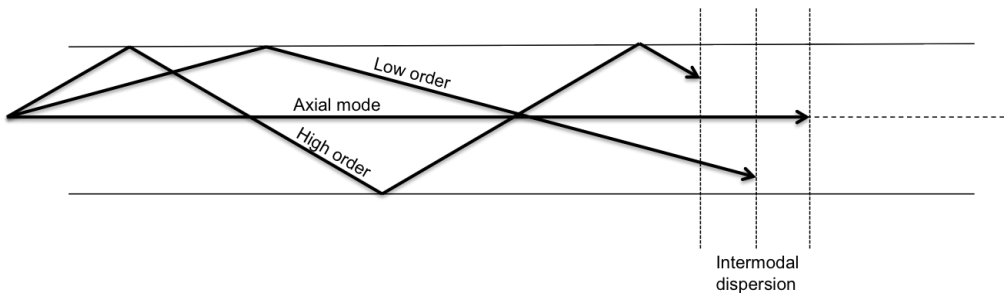


Figure 2.2: Higher modes take more time to reach a certain distance than the axial mode. The vertical dotted lines indicate the same time interval [8].

This is group velocity is given by the equation:

$$v_g = \frac{c}{n - \lambda \frac{dn}{d\lambda}} = \frac{\omega}{\beta} \quad (2.6)$$

Here n is the refractive index of the medium the light is traveling in, λ is the wavelength of the light and ω [s^{-1}] is the frequency. The propagation constant is given by β [m^{-1}]. This propagation constant of a medium can be expressed in terms of the *normalized* propagation constant b by

$$\beta = k \cdot \sqrt{n_2^2 + b(n_1^2 - n_2^2)} \quad (2.7)$$

where k [m^{-1}] is the wavenumber in vacuum in the form $\frac{2\pi n}{\lambda}$. The reason why this is expressed like this, is because b is empirically related to the V-number. The limits of b ($0 < b < 1$) is equal to $kn_2 < \beta < kn_1$ where n_2 is the refractive index of the cladding and n_1 that of the core. This shows that the group velocity is depending on several quantities of the fiber, such as the refractive indices of the core and the cladding and the fiber diameter [13].

The time difference that occur from this intermodal dispersion will usually be in the order of a couple of nano seconds per kilometre and will therefore not be important for the relatively short fibers that will be used.

2.2 Evanescent wave

We know that light can be seen as an electromagnetic (EM) wave, where the electric and the magnetic field are oscillating perpendicular relative to each other. The direction of propagation of the EM wave is given by the Poynting vector $\vec{E} \times \vec{B}$. The E-field of the EM-wave can be written in a complex form as

$$E = E_0 e^{i(k \cdot r - \omega t)} \quad (2.8)$$

where k is the wavenumber and r [m] is the position of the wave. The time is given by t [s] and ω [s^{-1}] is the frequency of the light wave.

Once the light wave is propagating in the fiber it will undergo total internal reflection when the reflecting angle is greater than the critical angle (see also figure 2.1)

$$\theta_r > \theta_c \quad (2.9)$$

With the help of the Fresnel equations it can be shown that in this case there will be no transmitting field present in the cladding.

This can be showed with the amplitude reflection coefficient, which is defined as

$$r = \frac{E_{r0}}{E_{i0}} \quad (2.10)$$

and will be equal to one for both the parallel and the perpendicular component of the incident light wave [9].

This can actually not be completely true. The Fresnel equations come with certain boundary conditions. One of them says that the tangent component of the E-field on one side of a surface must be equal to the E-field on the other side of that surface. (This is also true for the B-field, but since the interaction with the electric field is much stronger only the E-field will be taken into account).

This electric field is given by

$$\oint \vec{E} d\vec{l} = 0 \quad (2.11)$$

where the electric field is integrated over a certain distance l .

When there is an electric field on one side of the surface, one can draw an imaginary 2D Gaussian pillbox around that surface (see figure 2.3). Because an E-field is conservative around a closed path, the sum of the line integrals must be equal to zero since there is no net charge present in the fiber. So the integral for the E-field in this example becomes

$$\int_a^b E dl + \int_b^c E dl + \int_c^d E dl + \int_d^a E dl = 0 \quad (2.12)$$

Because the tangent of the E-field only moves in the z direction, there is no field propagating in the y direction. This gives

$$\int_a^b E dl + 0 + \int_c^d E dl + 0 = 0$$

$$E_{ab}\Delta z - E_{cd}\Delta z = 0$$

Which results in

$$E_{ab} = E_{cd} \quad (2.13)$$

This makes clear that there has to be an electric field on the other side of the surface, in this case in the cladding of the fiber [20].

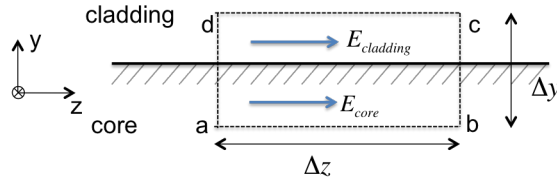


Figure 2.3: Imaginary Gaussian pillbox around a surface. The E field moves in positive z-direction

So, even if there is total internal reflection, there has to be a wave outside the core, but this wave cannot carry energy, on average, from the core in the cladding according the Fresnel equations. This is because r is still equal to one, so all the energy of the light wave have to be reflected.

In reality however, the size of the beam is not close to a plane wave, for which these equations a derived for. This means that the light can be diffracted as it propagates across the boundary into the second medium. When a third medium with a higher refractive index as the second medium (the cladding) is brought close, the evanescent wave can propagate to this third medium. The electric field that is carried across the border into the cladding, is equal to

$$E_t = E_{t0} e^{-\alpha y} e^{i \left(k_t \frac{\sin(\theta_j)}{n_1} x - \omega t \right)} \quad (2.14)$$

where α [m^{-1}] is the the attenuation coefficient in the y direction and k_t is the wavenumber for the transmitting wave ($k_t = \frac{2\pi n_2}{\lambda} = \frac{2\pi n_2 \cdot \omega}{v_p}$ with v_p the phase velocity) and ω is the frequency of the light wave moving in the z direction (see figure 2.4). The attenuation coefficient α [m^{-1}] can be derived from Snells law and some basic geometry to be

$$\alpha = \frac{2\pi n_2}{\lambda} \cdot \sqrt{\left(\frac{n_1}{n_2}\right) \sin(\theta_j) - 1} \quad (2.15)$$

This gives a standing wave, or evanescent wave, that is propagating in z and decays in the y direction [16]. The penetration depth δ [m] of the evanescent wave is given in

$$\delta = \frac{1}{\alpha} \quad (2.16)$$

The penetration depth is thus depending on the wavelength of the light, but also on the incidence angle. A smaller angle of incidence will increase the penetration depth, just as a larger wavelength. The depth that is calculated with this equation is where the wave is decreased by a factor $\frac{1}{e}$ [11].

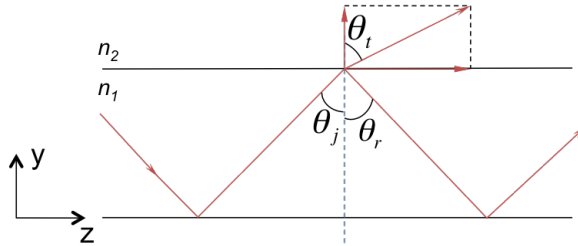


Figure 2.4: Evanescent wave penetrating in the cladding. Shown are respectively the incidence angle (θ_j) with respect to the normal, the reflection angle θ_r and the transmission angle θ_t with the two components.

The E-field of a light wave in a fiber is usually Gaussian distributed. This means that the optical power, or E^2 , is at its maximum in the centre of the core and is decaying exponentially towards the edge of the fiber.

The Gaussian distribution gives a power density of

$$E(r)^2 = E_0^2 e^{\left(\frac{-r}{w}\right)^2} \quad (2.17)$$

where E_0^2 is the optical power in the centre of the fiber core, r is the distance from the core and w is the distance from the core to the $\frac{1}{e^2}$ point of the Gaussian distribution (known as the mode field diameter or MFD) (see figure 2.5) [13]. The real shape of the light wave is not completely a Gaussian because the different refractive index from the cladding relative to the core deforms the shape. So the shape drawn in this figure does not continue like a Gaussian at the edge of the core but get refracted instead.

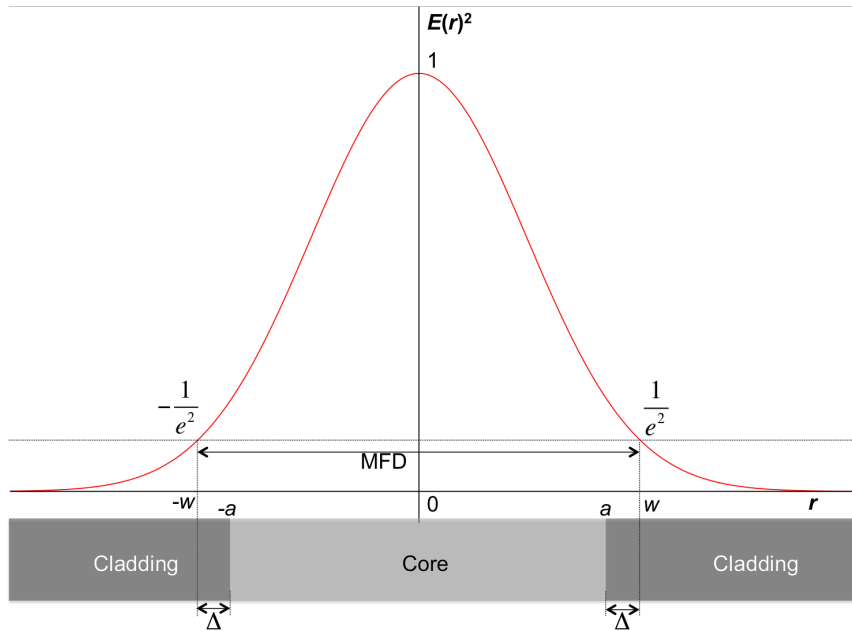


Figure 2.5: Mode field diameter of the fundamental mode with the dimensions of the fiber. The dark part of the fiber that is within the mode field diameter is the part where there will be an evanescent field present.

If the diameter of the core is smaller than the total width of the power density ($2w$), the field will exist outside the core and there is an evanescent field.

Because the V-number of the fiber is usually known, it is very useful to express the width of the power density in terms of the V-number (see equation 2.4).

This is done in the Marcuse MFD equation, which is

$$2w = 2a \cdot \left(0,65 + \frac{1,619}{\sqrt{V^3}} + \frac{2,879}{V^6} \right) \quad (2.18)$$

where $2a$ is the diameter of the core. This is an approximation and is only accurate when the V-number is in the range of $0,8 < V < 2,5$ [13]. The size of the field outside the core is the difference between the mode field diameter and the core radius, given in

$$\Delta = w - a \quad (2.19)$$

This equation does not take the refraction between the core and the cladding into account. The difference given by Δ is usually not bigger than a few λ , so evanescent coupling should be done within this range. The MFD according to equation 2.18 is equal to the inverse of the V-parameter. To increase the MFD, the guided wavelength can be increased or the diameter of the fiber can be decreased. Because optical fibers and connectors are designed for a specific wavelength (or small wavelength range), it will make more sense to decrease the diameter to control the evanescent coupling. Herefor the fiber will be tapered and, to make the coupling with optical devices easier, it will be dimpled afterwards [15].

2.3 Tapering a fiber

The fiber will be prepared for coupling by decreasing the diameter. This is the first step in the process for evanescent coupling using an optical fiber.

For this purpose the fiber needs to be as thin as possible to make Δ as large as possible because the evanescent wave is decaying relatively fast in the y-direction.

Tapering a fiber is done by heating the fiber and subsequently stretching it, so the fiber will become longer. Because of the conservation of matter, the diameter of the fiber decreases.

The heated part of the fiber, or the hot-zone, becomes the weak spot and that is where the diameter decreases as a function of time. Because only a small part of the fiber is heated, the tapering occurs only in a region of maximal a couple of millimeters.

When the fiber is stretched, the initial diameter of the fiber d_0 [m] decreases as a function of pulling time t [s] and speed v [m s⁻¹]. This diameter can be calculated to be

$$\begin{aligned} d_1 &= d_0 e^{-(vt)/L_{hz}} \\ &= d_0 e^{(-x/L_{hz})} \end{aligned} \quad (2.20)$$

Where L_{hz} is the hot-zone length [m] and x is the pulling distance which is $x = vt$. See appendix A for a derivation of this equation [6] [7].

Figure 2.6 shows the general idea of a tapered fiber.

Because the diameter of the tapered region is related to the V-parameter, the time after the fiber becomes single mode can be derived by simply insert equation (2.20) in equation (2.4). With $d = d_1$ this gives

$$V = \frac{\pi d_0}{\lambda} e^{(-x/L_{hz})} \cdot NA$$

where x can be isolated to give

$$x = vt = -L_{hz} \cdot \ln \left(V \cdot \frac{\lambda}{\pi d_0 NA} \right) \quad (2.21)$$

When there are multiple modes present in a fiber, each of those modes can interfere with each other. When the fiber is getting pulled and the diameter decreases, the number of modes that will exist in the waveguide will also decrease, according to equation (2.5).

It can occur, for example, that two rays of light destructively interfere and therefore cancel each other out. As the fiber is getting pulled, one of the rays can, at a certain point, not propagate through the fiber anymore and stops to interfere with the second light ray. This second ray will not interfere destructively anymore, and can now propagate through the fiber and contribute to the output signal. If the fiber continues to decrease, eventually this ray will also be blocked. This process causes oscillations as a transmission profile that is expected during the tapering process.

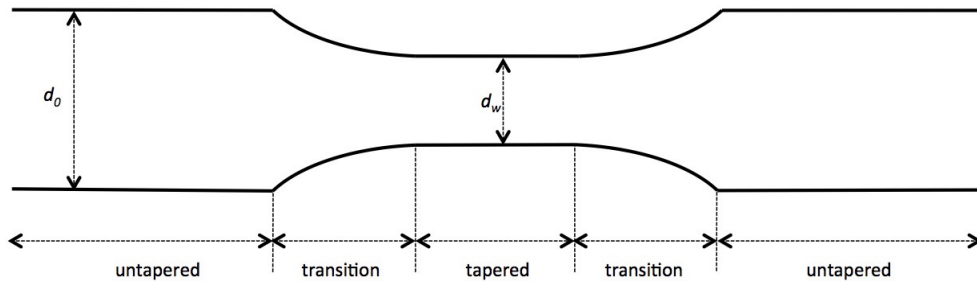


Figure 2.6: Schematic representation of a tapered fiber with the different regions.

The frequency of these oscillations is expected to increase as the pulling speed increases, as consecutive modes are being extinguished faster than with a lower pulling speed. When these oscillations stop there is only one (the axial) mode propagating in the fiber and so it is single mode [17]. These oscillations give an indication when a fiber is becoming single mode, but also about the quality of the fiber. A fiber with a lot of damages will have a lower transmission efficiency relative to a fiber with no damages. A standard fiber, like for instance a SMF-28, have an attenuation of $\gamma \leq 0,20$ dB/km at a wavelength $\lambda = 1550$ nm. This attenuation is defined as the ratio between the input and output power

$$\gamma = 10 \cdot \log_{10} \left(\frac{P_{in}}{P_{out}} \right) \quad (2.22)$$

where P_{in} and P_{out} are the input and output power [W] respectively. For the short fiber lengths that will be used this will not give any visible losses of optical signal. So, the losses that occur during pulling will most likely come from the damages in the fiber where light can scatter off and bendings where light can be refracted out the fiber.

2.4 Heating a fiber

The fiber will initially exist as a core and a cladding with each a different refractive index. To control how a material affects light, the basic material of the fiber is doped with a second element. Most fibers are made from silica and are doped with a specific element in order to lower or raise the refractive index.

Because the core and the cladding are based on the same material, the melting temperatures are both almost the same. The flame temperature needs to be around the melting point of the silica in order to make the fiber soft enough so it can be pulled.

This means that the core and the cladding can melt together, creating one core with a diameter of the initial cladding before heating. In this new bigger core, the light is confined because of the difference of refractive index between the fiber and the air.

If the core and the cladding are melted together, the refractive indices are not immediately equally distributed within the fiber. This causes the light to follow non-linear paths as it propagates through the hot-zone and the transition region of the fiber. While the fiber is getting thinner, the concentration of the doping, and therefore the refractive index, becomes more evenly distributed.

2.5 Dimpling a fiber

Once the fiber is pulled, it can be dimpled to more precisely control the location of optical coupling. The tapered region of the fiber has typically a length of several millimetres. The evanescent field will extend the fiber all over the tapered region, and so coupling can occur over a relatively large distance. To control the location of the coupling, a small dimple will be made in the tapered fiber. Only a small part of the tapered zone will then come close enough to the target where the light needs to be transferred to.

The dimple shall typically be made with a rod with a diameter of maximal around hundred micron. Because of the small diameter of the rod, the fiber will exceed the maximum bending radius. The light in the fiber is partly propagating in the cladding of the fiber. When the fiber is bent, the light wave has to turn in with the bending radius. The part of the light wave that is in the inner corner of the fiber has to travel a smaller distance than the part in the outer corner in the same time interval to stay in phase with the rest of the wave. The outer part must therefore increase its speed. When the fiber is bent severely, the part of the wave that is in the outer corner has to travel faster than the speed of light in vacuum, so $v_g > c$. Since this is not possible, that part of the wave will be radiated away and is assumed to be lost. The losses increase exponentially with the bending radius. For multimode fibers, the losses are usually higher in comparison with single mode fibers, because higher modes are penetrating more in the cladding than lower order modes.

During the dimpling, the signal is therefore expected to drop to zero, as the fiber is not able to keep the light trapped in the fiber. After the dimpling rod is released, the dimple in the fiber will relax and the radius of the curvature decreases. This leaves a small dimple in the fiber with a curvature lower than the maximum radius of curvature, so the losses should remain to a minimum (i.e. a few per cent). When not dimpled properly, it can cause micro bends where the light can scatter off resulting in a lower transmission after dimpling (see figure 2.7 right). Especially because the dimple is made in the tapered region where there is no protective coating around the glass. This coating usually ensures the performance of the fiber, also when small defects are present in the glass.

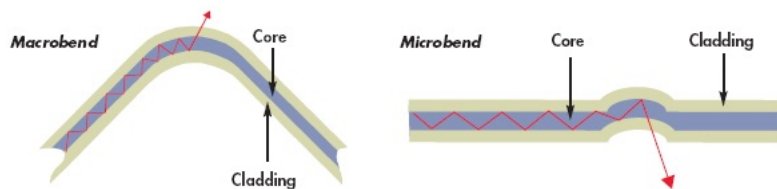


Figure 2.7: **Left:** macrobends losses as can occur during the dimpling process. **Right:** Small microbends can after the dimpling procedure cause permanent losses in the fiber [25]

3 Experimental Set-Up

The set-up will be verified by tapering several fibers to find the best values for the different parameters.

The fiber that is going to be used for the experiment is a basic fiber that is mostly used for optical communications. This is a CORNING SMF-28e+ optical fiber with a core diameter of $8,2 \mu\text{m}$, cladding diameter of $125 \mu\text{m}$ and a numerical aperture of $0,14$. The core has a refractive index of $n_1 = 1,4679$ and $n_2 = 1,4612$ at $\lambda_t = 1550 \text{ nm}$. (Both the core and the cladding are made from silica, which are doped differently).

With this, the fiber has a V-number at λ_t equal to $2,3268$, indicating that is single mode.

In figure 3.1 is the size of the optical field, the mode field radius w , shown as a function of the core diameter at two different wavelengths with equation 2.18. The dotted lines give the size of the field outside the core (Δ) for the two wavelengths (see equation 2.19).

The graph is only plotted in the range of $0,8 < V < 2,5$ where the equation is valid. For example, for the initial radius of the core ($4,1 \mu\text{m}$) the mode field radius is $w = 4,61 \mu\text{m}$. The radius of the field outside the core is about $\Delta = 0,51 \mu\text{m}$, what is still in the cladding of the fiber which extends to $62,5 \mu\text{m}$ from the centre of the fiber.ⁱ

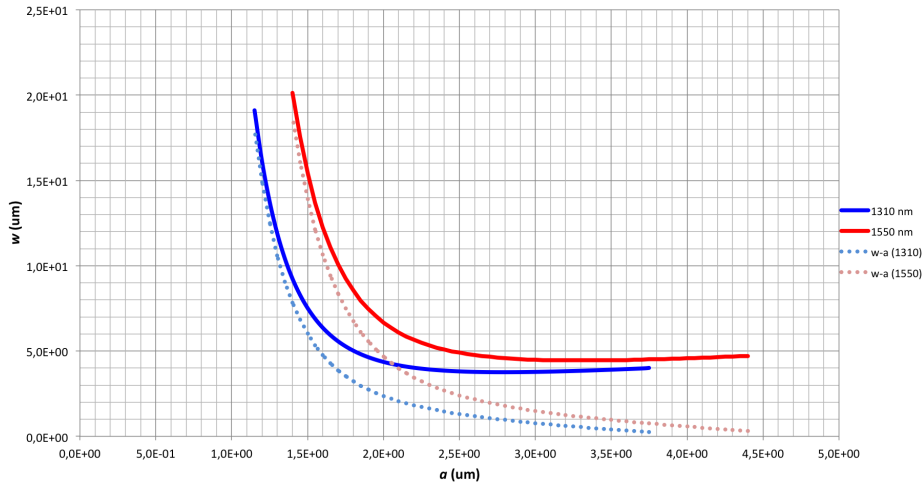


Figure 3.1: w as a function of a . Marcuse MFD equation for a SMF-28e+ optical fiber for $\lambda = 1310 \text{ nm}$ and $\lambda = 1550 \text{ nm}$ in the range $0,8 < V < 2,5$. The dotted lines give the distance of the field outside the core with equation 2.19 (Δ as a function of a).

ⁱThis is not plotted for the situation where the core and the cladding are melted together. Because of the relative large difference between the refractive index of the fiber and the air, the V-number becomes very large. The diameter of the fiber needs to be chosen small (order of magnitude of around hundred nanometre) to keep the V-number within the range where the Marcuse MFD equation is valid.

With equation (2.21) and the parameters of the fiber, the theoretical pulling length when the fiber becomes single mode can be estimated. It is assumed that a V-number less or equal to 2,4048 corresponds to a single mode transmission. Because after heating and pulling for a short time, the light is guided in the cladding of the fiber instead of the core. So, the initial diameter of the fiber is the diameter of the cladding, $d_0 = 125\mu\text{m}$. The refractive index of the core where the light is guided in is 1,46 and the cladding is air with $n = 1,00$. For a wavelength of $\lambda = 1550\text{nm}$ and a hot-zone length of 4mm, the total elongation length of the fiber where it becomes single mode is equal to 18,8mm. This is at a diameter of the tapered regio around $1,2\mu\text{m}$. What will be the expected pulling length and diameter of the fiber at 1550nm.

For a smaller hot-zone, the elongation length that is needed for the fiber to become single mode shall also be smaller. But this also causes the transition region to become shorter which can cause lower transmission efficiency as the light is getting less gradually guided from the thick part to the tapered region of the fiber. In figure 3.2 is a semi-logarithmic plot shown of the diameter as a function of pulling distance for several different hot-zones. The initial diameter is $d_{smf} = 125,0\mu\text{m}$.

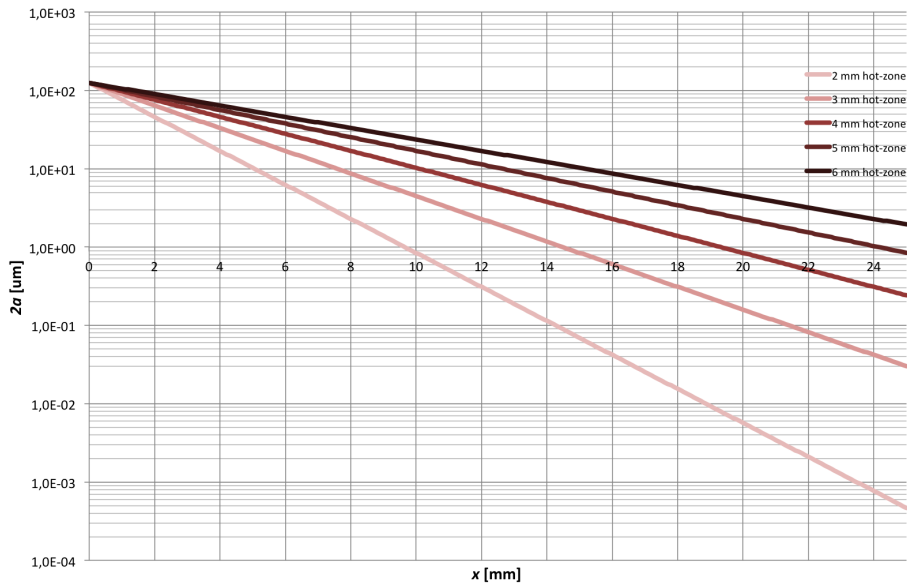


Figure 3.2: Fiber diameter as a function of pulling distance for several different hot zones between 2mm and 6mm. The initial diameter is $125,0\mu\text{m}$. The vertical axis is the diameter and is plotted in logarithmic scale.

3.1 Preparations for tapering

The fiber is covered in an acrylate coating to protect the glass. This disturbs the heating process of the fiber, so this coating is removed by using a Thorlabs FTS4 three-hole stripping tool. After stripping, the fiber only exists as a core and a cladding at the area that is going to be heated. The fiber can now directly be heated using a hydrogen flame, mainly because hydrogen burns clean and has a high enough temperature to melt the glass. This is controlled with a National Torch HT-3 torch tip and a flow meter. To keep the flame as stable as possible, an enclosure is placed around the setup to prevent the flame from moving due to air flow. The hottest part of the hydrogen flame is around the edge. The centre of the flame is not hot enough to heat the fiber up as much as is necessary to melt the fiber. If the fiber is placed through the middle of the flame, it would therefore generate two hot zones and as a result there will be two tapered regions. This is not ideal, so the fiber is placed at the edge of the flame to make one continuous tapered region. The fiber has a melting temperature around 1500K to 1800K (depending of the doping concentration of the core and the cladding). The hydrogen flame has a maximum temperature of around 1937K with air as oxidizer [22].

The fiber is stretched to taper the hot zone. For this, the fiber is placed between clamps which holds the fiber firm enough to prevent it from slipping. These clamps are placed on two Suruga Seiki kxl06100-N2-GA stages. These have a maximum traveling distance of 100mm and a speed range of $0, 1 < v_s < (30 \cdot 10^3) \mu\text{m s}^{-1}$. The resolution of the speed is $0,1 \mu\text{m s}^{-1}$. The torch is placed on a Suruga Seiki kxl06050-N1-CA stage, which has a traveling distance of 50mm. The specifications are similar to those of the 100mm pulling stage [23].

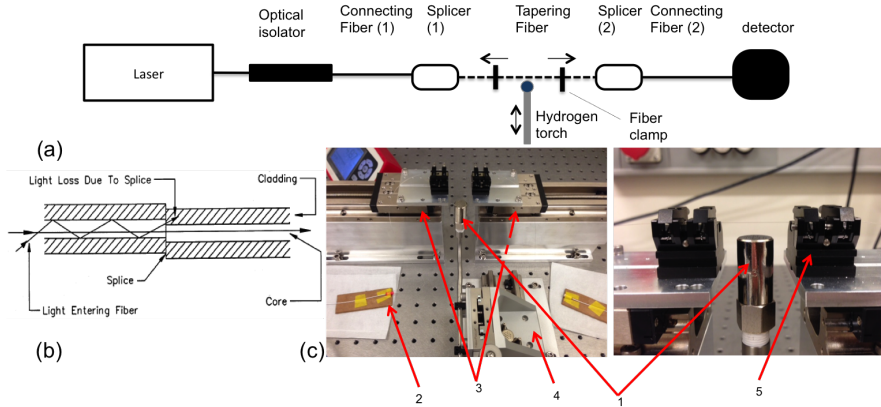


Figure 3.3: (a): Schematic overview of the set up. The fiber clamps are each mounted on a stage. (b): Schematic representation of the splicer when the fibers are not perfectly aligned [26]. (c): Used setup for the described experiment. 1; HT-3 torch 2; one of the splicers with the white connecting fiber 3; Suruga Seiki kxl06100-N2-GA pulling stage 4; Suruga Seiki kxl06050-N1-CA torch stage 5; fiber clamps with a fiber placed.

The pulling stages are moving in opposite direction relative to each other and the torch stage is placed orthogonal on the pulling stages. The stages are programmed so that the pulling stages start tapering the fiber after the torch is moved under the fiber. If wanted, there can be a delay introduced so that the fiber can heat up before the tapering begins.

To measure the transmission, light is coupled in the fiber by using a NewFocus 6427 laser with adjustable wavelength in the range $1500 < \lambda_{NF} < 1575$ nm. The fiber that is being tapered cannot directly be coupled in the laser. A second fiber is plugged in the laser on one end and the other is placed in an elastomeric lab splicer. These mechanical splicers form a link between the fiber from the laser and the tapering fiber. The fiber ends needs to be stripped from the protective acrylate coating with the stripping tool. Because the ends of the fibers will simply be placed together in the splicer, the ends also needs to be cleaved to keep losses as low as possible. These straight cuts are made using a Fujikura CT-30 fiber cleaver. After this the fiber needs to be cleaned using alcohol and matching gel is applied to the ends to minimize losses.

This matching gel has a refractive index close to that of the fiber where the light needs to be coupled into. When there is a mismatch between the refractive indices of the fibers, a part of the light is being reflected or refracted. This matching gel should minimize the loss that occurs from this difference. This procedure is done for all the fibers that are connected with a splicer, that is the connecting fiber from the laser with the optical isolator (this will be discussed later), the tapered fiber and the connecting fiber to the detector. With these splicers the losses, due to for example misalignment, should remain below $\gamma_{splicer} = 0,5$ dB per splicer. (See figure 3.3b.)

The transmission of the light is measured with a Thorlabs PM100D power meter with a S154C InGaAs photo detector. This photo detector has a power range between $-80 < P < +5$ dBm where the output power is defined by

$$\begin{aligned} P_{dBm} &= 10 \cdot \log_{10}(P_{mW}) \\ &= 30 + 10 \cdot \log_{10}(P_W) \end{aligned} \tag{3.1}$$

where P_{mW} is the power in milliWatts and P_W is the power in Watts.

In addition a camera with a microscopic lens (maximum 100x magnification) is used to check by the quality of the fiber by eye and measure directly the diameter.

Once the fiber is prepared by stripping and splicing and is placed in the clamps, the torch is lit. To keep the fiber clean from dirt from the lighter, a sheet of metal is placed to isolate the fiber from the torch when lit.

3.2 Preparations for dimpling

Before a dimple will be made in the fiber, it will be bended so it is easier to handle and better to control during the evanescent coupling. The fiber is released from the tapering setup and will be placed on an in-house made device where the fiber is bended in an U-shape. Because the thinner part of the fiber is more likely to bend than the thicker part, it probably will not be a perfect round curvature, but instead have a little shaper curvature around the tapered region.

After bending, the complete device with the fiber will be placed in a second set up. This set up consists of a manually controlled xyz-stage where the bending device with the tapered fiber is mounted on and a second hydrogen torch that is also mounted on a xyz-stage. These stages are for precise placing of the fiber and the torch relative to the stationary dimpling rod.

The dimpling rod is another piece of SMF-28e+ fiber where the acrylate coating is stripped off for creating a dimple with a radius of $125\ \mu\text{m}$. Because the fiber and the dimpling rod are heated, there is a great chance that the two fibers will stick or melt together (both are the same material). To prevent this, the dimpling rod is covered in a small layer of graphite powder (Kasp K30050 Microfine graphite powder). Small amounts of graphite will burn off during heating, but if used too much, it can leave some residue on the tapered fiber. This can be removed using compressed air to blow of some of the graphite powder.

The second hydrogen torch is mounted with a smaller torch tip. Only a small flame is needed to heat the dimpling rod in comparison with the tapering process where a large flame is desired for a large taper region. The torch is placed under the dimpling rod to heat it up. The tapered fiber is placed between the dimpling rod and the torch and, while heated, moved up to create a dimple. The dimple in the tapered fiber will be only tens to hunderds of microns high. It will be empirical determined what the best dimpling distance and time is (i.e. how far the tapered fiber will be moved upwards and for how long), depending on the transmission loss after the dimpling (See figure 3.4).

During the dimpling the transmission will drop to zero because the maximum radius of curvature will most likely be exceeded. After the dimpling rod and the tapered fiber are separated again, the tension will drop from the tapered fiber. This decreases the radius of curvature, allowing light to be guided through the fiber again while leaving a small dimple in the fiber. With this setup, a loss of only a few per cent should be possible to maintain.

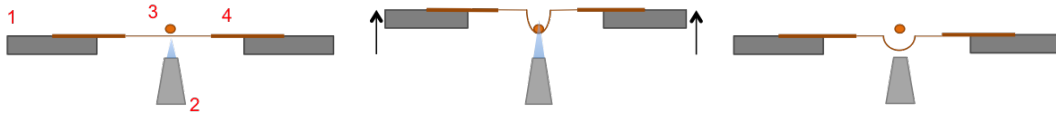


Figure 3.4: Front overview of the setup. Bending device with the tapered fiber moves up to the dimpling rod while it is heated. This leaves a small dimple in the tapered region.

1; Bending device **2;** Hydrogen torch **3;** Dimpling rod **4;** Tapered fiber.

3.3 Validation

For measuring the transmission of the laser during pulling, the fiber is coupled to a New-Focus 6427 laser. This laser has an adjustable wavelength what is necessary for checking the quality and some device parameters of the optical resonators. For the fiber pulling a constant wavelength is used of $\lambda_{pull} = 1550$ nm. To check the output signal of the laser, it is directly coupled in the detector using a standard non-tapered fiber. When the laser is turned on, it should provide a stable output power, but the laser output shows instead some fluctuations. This can be the cause of optical feedback in the laser due to reflections. The laser was set to 0,0dBm for a time period of 1000s. The peak-peak value of the transmission is normalized to the initial power at $t = 0$ with

$$P_{norm} = (10^{P_{out}-P_{in}})^{\frac{1}{10}} \quad (3.2)$$

where P_{out} and P_{in} are measured in dBm and P_{norm} is the normalized power in mW. First this is measured for a normal fiber with a measured start attenuation of 0,288 dB. (See figure 3.5a).

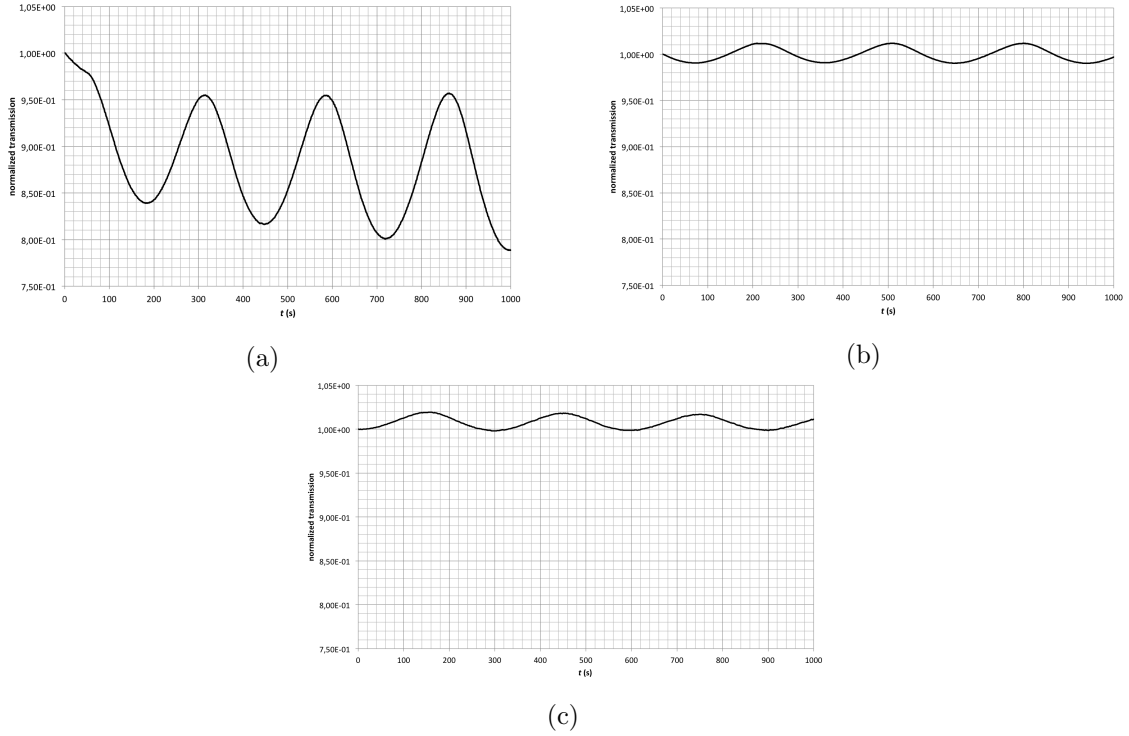


Figure 3.5: **a:** Relative fluctuations of the output power of the laser as a function of time without an optical isolator. **b:** Relative fluctuations of the output power of the laser as a function of time by using a fiber with an optical isolator. **c:** Relative fluctuations of the output power of the laser as a function of time by using a fiber with an optical isolator and the splicers, similar to the tapering setup.

The signal shows a relative change of approximately 11%, but is slowly increasing to about 16% in this time period. The period of the oscillations is almost constant at $\tau = 270$ seconds.

To minimize the feedback of light into the laser, an optical isolator is introduced in the system. This is a polarization insensitive faraday rotator that works with a birefringent crystal shaped in a wedge form. This separates the perpendicular components of the light wave. The faraday rotator rotates each of the components by 45° . A second birefringent wedge, with the fast- and slow axis at 45° and -45° respectively, combines the components again. When the light is reflected back into the isolator, the second wedge separates the components, but after the rotator the first wedge diverge the components even further and the light wave shall not continue its way back [28]. The isolator causes a bigger optical loss between the laser and the tapering fiber, but it provides a more stable signal. The initial attenuation is increased to about 0,848 dB, but the change in the signal is smaller with a peak-peak value of about 2%. The oscillations are constant with a period of $\tau = 290$ s (see figure 3.5b).

Last, the complete setup as will be used for tapering the fiber will be tested. This includes the optical isolator and the splicers with a stripped SMF-28e+ fiber in between. This is shown in figure 3.5c. The amplitude is still reduced to about 2% with a slightly increasing period in the range from 280s to 320s. The amplitude is small enough to be ignored during the measurements.

The transmission losses between the laser and the tapering fiber come mostly from the optical isolator, the splicers and the connecting fiber.

The two splicers have a maximum loss of 0,5dB each at a perfect splice and the optical isolator has a loss (due to imperfections of the antireflection coating for example) of about 0,45dB. The connecting fiber has an insertion loss of $\leq 0,08$ dB.

The fiber with the optical isolator is connected to the fiber that is spliced with the tapering fiber. This connector (A Seikoh Giken SNA-1 optical connector) has a maximum loss of 0,2 dB. The tapering fiber, which is about 1m before pulling, has a attenuation of about $2,0 \cdot 10^{-4}$ dB m^{-1} at $\lambda = 1550$ nm. This is relatively small in comparison with the other losses of optical signal.

This sums up the insertion loss of the fiber that is connected to the laser, the loss from the optical isolator, the connector, and the two splicers.

This gives a maximum loss of $\gamma_{sys,max} = 1,73$ dB for the system. It is a rough estimation and in practical a transmission loss can be minimized to about 1,5dB depending on the quality of the splicing.

As mentioned before, the fiber can contain damages, which causes the fiber to break easily or give a lot of losses. It can be checked by eye with the use of the microscopic lens if a fiber is damaged. In figure 3.6a, a fiber is shown at a point where the fiber is not tapered yet and contains no (serious) damages. In figure 3.6b is a tapered transition region shown with micro cracks. In this case it is probably caused by a wrongly use of the stripping tool.

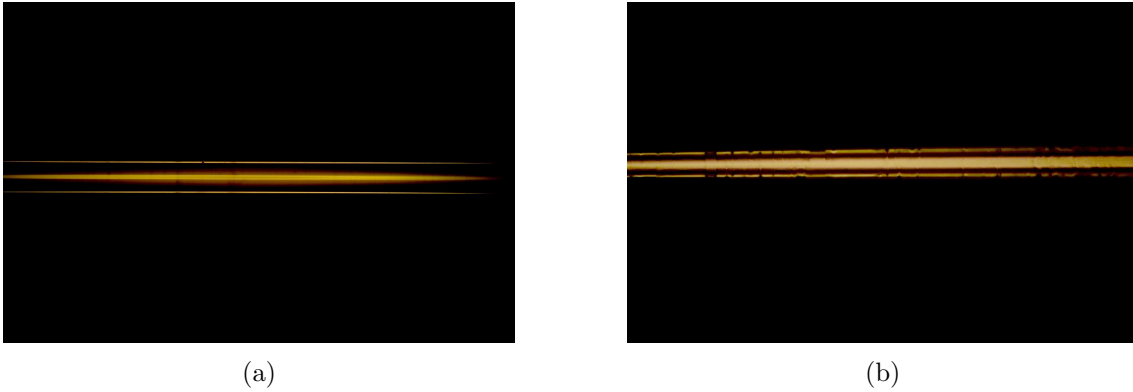


Figure 3.6: **a:** Microscopic image of a SMF28e+ fiber without damage. Visible are the cladding and the core. **b:** The fiber with damages (The white balance and contrast of this image is slightly changed to make the damages better visible. That is why the core appears to be bigger).

4 Transmission measurements

The previous described tapering set up is used to decrease the diameter of several fibers. The initial length of the fibers is usually around one meter. This is chosen relatively long so that there is only a little to no force acting on the splicers. If short fibers are used, the splicers have to be placed on the moving stages and so there will be a force present because the splicers will move relative to the laser and the detector. This can affect the coupling and therefore disturbing the transmission that is measured during pulling. Also the fiber is taped down on the table. This ensures minimal movement of the fiber within the splicers.

Several different parameters can be set for the stages. The most significant are the driving speed and the time delay between the start of heating the fiber and the start of pulling. This gives the hot-zone time to heat up and get softer before the fiber is tapered. Also the acceleration rate can be set. This is the time it takes for the stages to reach the driving speed given in milliseconds.

The acceleration rate is not as significant as the driving speed and the delay time, but the acceleration is introduced to prevent damaging the fiber due to sudden tensioning the fiber as the pulling stages start to move. Before the fiber is heated, it is slowly pre-tensioned so that the fiber is straight between the clamps. This should prevent bends in the fiber after it is tapered.

The position of the torch-stage is empirical determined by looking by eye what the best position is. This can be seen as the hot-zone of the fiber lights up as it is getting heated. Important is to check if there is only one hot-zone present.

4.1 Transmission efficiency during pulling

Several different settings has been tried to check which gives the highest transmission and best reproducibility.

The order of magnitude for the driving speed is around tens of micrometres per second. This is comparable with others papers like [6] and [7].

Higher speeds has been tried (for example $100\mu\text{m s}^{-1}$ and $240\mu\text{m s}^{-1}$), but that seems to damage the fiber, causing it to break before it becomes single mode.

The best results are between speeds of $30\mu\text{m s}^{-1}$ and $50\mu\text{m s}^{-1}$.

For the $30\mu\text{m s}^{-1}$ speed, the fiber needs around 350 to 490 seconds before it will become single mode. For a speed of $50\mu\text{m s}^{-1}$ this fluctuates around 190 to 250 seconds.

In figure 4.1 the transmission is shown of a pulling at $40\mu\text{m s}^{-1}$ with a acceleration time of $t_{Acc} = 500\text{ms}$ at a wavelength of $\lambda_{pull} = 1550\text{nm}$ and a delay time of 5 seconds for pre-heating the fiber before pulling.

The multimode oscillations start at around 85 seconds and the fiber becomes single mode again after pulling for a total of 400 seconds. For calculating the taper length of the fiber, the total *pulling* time needs to be taken into account.

This means the time until the fiber becomes single mode for the second time minus the delay time (t_{delay} [s]). This gives

$$\begin{aligned} L_{pull} &= v \cdot (t_{pull} - t_{delay} - t_{post}) \\ &= v \cdot (t_{sm} + t_{mm}) \end{aligned} \quad (4.1)$$

This gives a pulling length of $40 \cdot 10^{-6} \cdot (440 - 5 - 40) = 40 \cdot 10^{-6} \cdot 395 = 15,8\text{mm}$. According to equation (2.20) the calculated radius of the fiber is at this point $r = 2,41\mu\text{m}$ by a hot-zone of 4mm.

The error made by calculating the pulling length of the stages, is depending of the uncertainty of the pulling time where the fiber becomes single mode and the error of the driving speed of the stages.

This can be determined with

$$\frac{\Delta L_{pull}}{L_{pull}} = \frac{\Delta v}{v} + \frac{\Delta t}{t} \quad (4.2)$$

Where $\Delta v = 0,1 \cdot 10^{-6} \text{ m s}^{-1}$ and Δt is the error made in determining the time where the fiber becomes single mode. In this example the error in the time is estimated about 3 seconds, giving an error in the pulling length of $\Delta L_{pull} = 0,16\text{mm}$ or about 1,0% of the calculated pulling length.

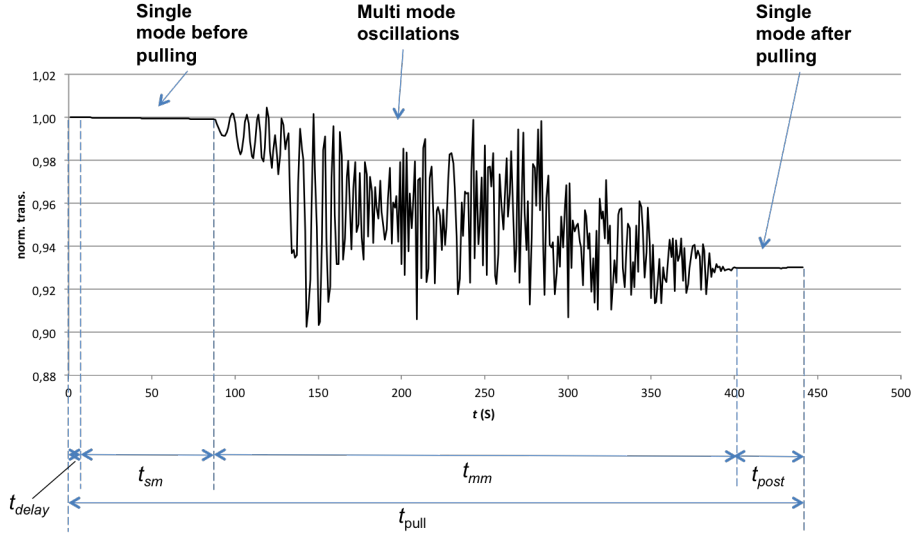


Figure 4.1: Plot of a fiber tapered with a speed of $40\mu\text{m s}^{-1}$. Shown are respectively the delay time, the time where the fiber is initially single mode, the time where the fiber is multi mode, time where the fiber is pulled after it becomes single mode and the total pulling time.

In figure 4.2 is the plot shown for a measurement done with a pulling speed of $30\mu\text{m s}^{-1}$. It takes the fiber about 70 seconds to become single mode. At that point the core and the cladding are melted together so that the light can escape from the core and be guided in the initial cladding of the fiber. Now multiple modes are allowed in the fiber and the interference of these different modes causes the signal to oscillate. After pulling for 410 seconds the oscillations stop and the fiber is therefore assumed to be single mode again. The pulling length according to equation 4.1 is 12,2mm. The diameter of the fiber at this point can be calculated using equation 2.20. The length of the hot-zone is estimated to be around 4mm in this example which results in a diameter of the tapered region of $5,9\mu\text{m}$.

The frequency and amplitude of the oscillations is not constant in time. This can be the result of the doping concentrations that are not immediately evenly distributed in the hot-zone. This changes the way that a light path interferes with another light path over time.

These measurements are repeated for different pulling speeds. The transmission efficiency as a function of elongation length has been plotted in figure 4.3. Different driving speeds of the pulling stages has been tried to show which one gives the best and most repeatable results.

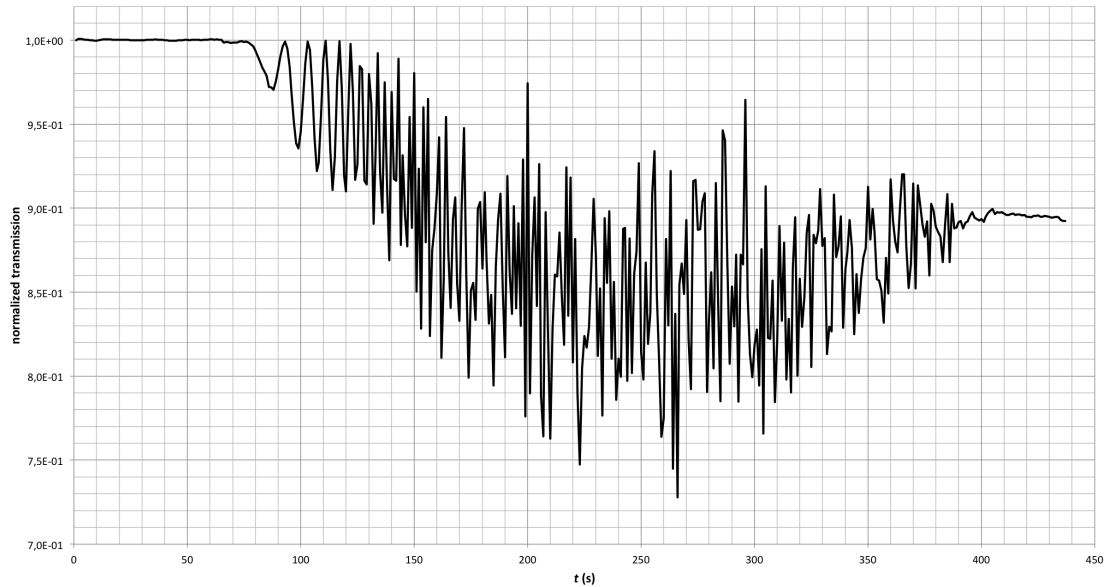


Figure 4.2: Transmission power as function time at a pulling speed of $30\mu\text{m s}^{-1}$ and an acceleration of 500 ms. The fiber has an efficiency of over 89%. The transmission is normalized to the initial input power.

The best transmissions are at a pulling distances larger than 12,0mm. A relative long pulling length gives a large transition region whereby light is gradually guided to the thinnest part of the fiber. This gives the lowest losses so that the average efficiency is bigger at longer pulling lengths. For pulling lengths higher than 12,0mm, the average efficiency is 85% for all the speeds. For pulling lengths lower than 12,0mm the efficiency is reduced to almost 70%.

The $30\mu\text{m s}^{-1}$ speed gives the highest transmission with an average of 78% but and the highest average pulling length of 12,4mm. The shortest pulling length, on average, is with a speed of $50\mu\text{m s}^{-1}$ with 10,9 mm with a efficiency of 76%.

At a speed of $40\mu\text{m s}^{-1}$, the pulling length of the stages are on average 11,9mm with an average transmission efficiency of al little over 75%. The averages of the different speeds are close to each other and for a statistically more reliable result, more measurements should be done.

The reason that the measured pulling length is not constant around a certain value is probably the unknown hot-zone length. This can vary a little and give a relative large difference in the diameter of the tapered region, because of the exponential decrease. This causes the fiber to reach its single mode diameter at different pulling lengths. For each measurement shown in the graph, the error is determined with equation (4.2). The error made in the time is most significant. For some measurements the time where the fiber becomes single mode is not as easy to determine (for example because of large fluctuations in the output signal in comparison with the final multi mode oscillations), resulting in a larger error.

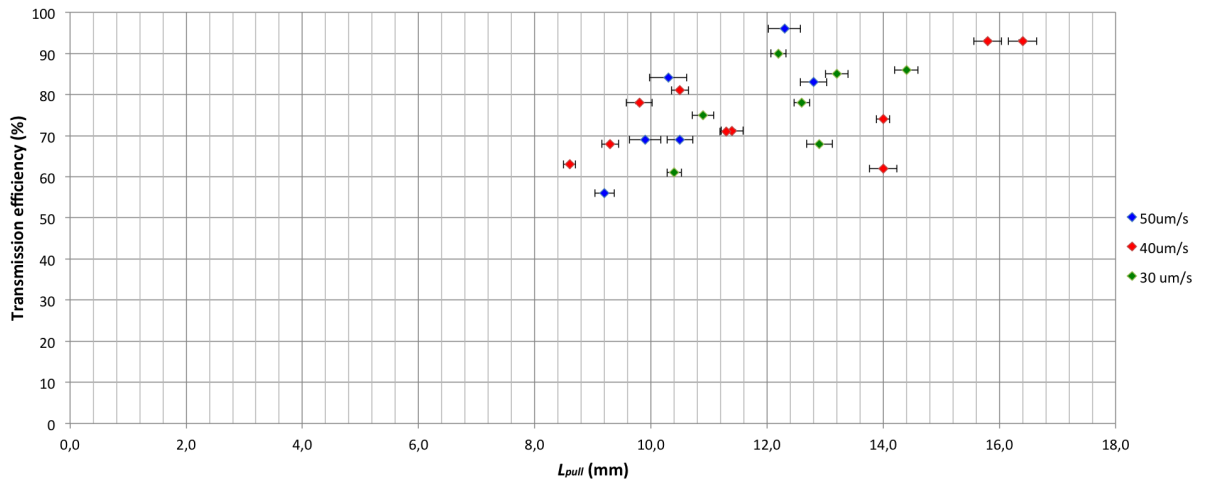


Figure 4.3: Transmission efficiency as a function of elongation length for different pulling speeds with errorbars.

4.2 Tapering diameter

Important is to get a consistent pulling length (i.e. a constant diameter of the tapered region) for each of the different speeds. This can be improved by stabilizing the signal, the hydrogen flame and the splicers as much as possible. Especially the flame needs to be constant, because during the experiments this is proved to be an important factor for a reproducible and good tapering result. Also the fiber should not slip between the clamps. When the fibers are taking care of properly and the setup is isolated as much as possible from for example air currents, the tapering should get more stable in comparison with the previous measurements. Also, the use of a microscope with a maximum of a 100x magnification allows measuring the fiber instead of calculating this diameter. This should improve the accuracy of determining the diameter. Any differences in, for example, the hot-zone was not taken into account in the previous method when the diameter was only calculated. In the figures below is an example shown of a tapered fiber and a reference fiber with a diameter of $125\mu\text{m}$. Also the edge detection is shown, where the two vertical red arrows in the green boxes indicates the edges of the fiber (see figure 4.4c and figure 4.4d).

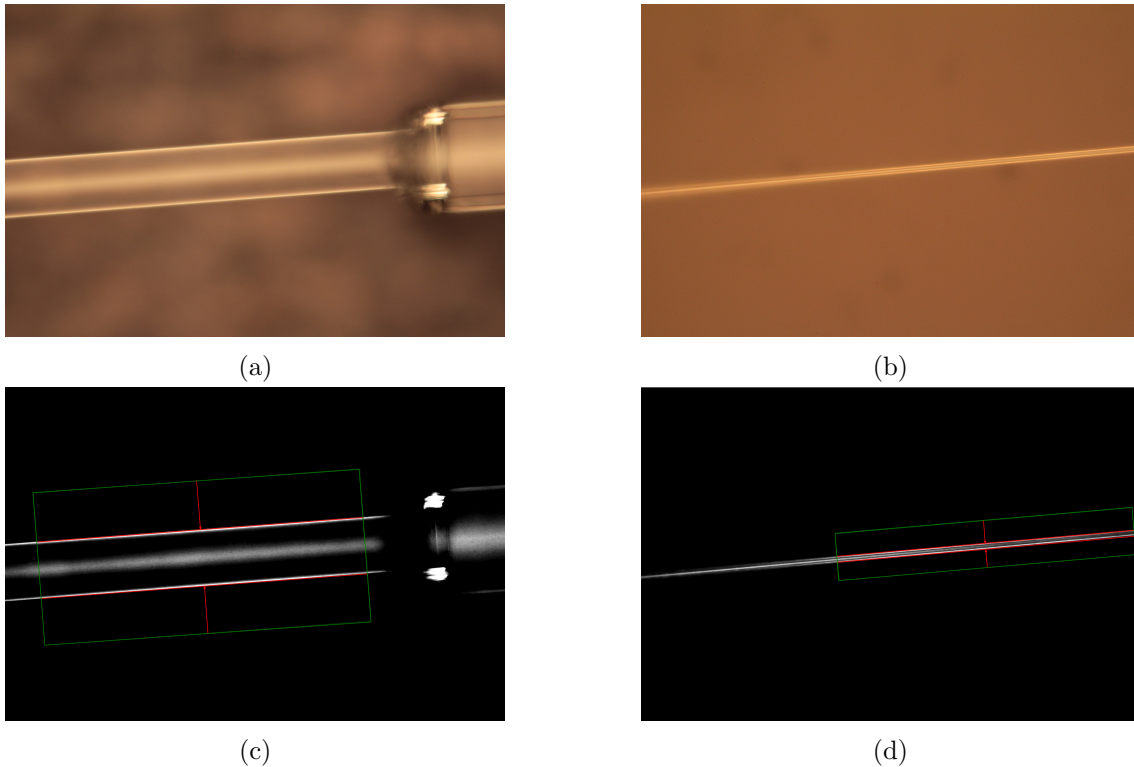


Figure 4.4: **a:** Microscopic image (20x zoom) of the non-tapered reference fiber with the diameter of $125\mu\text{m}$. On the right is a part of the acrylate coating visible. **b:** Microscopic image (100x zoom) of the tapered region of the fiber with a diameter of $2,8\mu\text{m}$. **c:** Reference fiber with the boundaries of the edge detection. **d:** Tapered region with the boundaries of the edge detection.

The diameter of the fiber can be determined using the ratio between the measured tapered diameter and the initial diameter. This ratio should be equal to the ratio of the real diameters of the fiber. The magnification of the microscope is known, but any magnifications of the image taken by the camera are not. By using a ratio, the magnification of the camera is not of any interest anymore. This ratio can be expressed in

$$\frac{l'_0}{l'_1} = \frac{d_0}{d_1} \quad (4.3)$$

Where l'_0 and l'_1 are the measured diameters of the reference and the tapered fiber respectively divided by the zoom level of the microscope. The l'_0 and l'_1 are measured and d_0 is the initial diameter of the fiber and d_1 is the real tapered diameter of the fiber.

The setup that was used is recalibrated and the hydrogen torch is realigned with the fiber when it is placed between the clamps. This improved the pulling so that the average transmission efficiency increased and get more stable. The transmission efficiency of the fibers as a function of the measured diameter is shown in figure 4.5. The diameter of the fibers is still not as constant as expected. At some of the measurements, the time when the fiber is becoming single mode is not always as easy to determine, probably because the fiber is not always aligned well enough before the pulling. Because of this, some of the fibers are getting pulled a little longer (or shorter in some cases) causing it to become thinner (or left thicker) than other fibers.

Most fibers are getting single mode between $2\mu\text{m}$ and $2,5\mu\text{m}$. This is thicker than initially expected in chapter 3. The pulling length is with all the measurements shorter than calculated, which automatically gives a larger diameter of the tapered region. The hot-zone of the fiber is on average between 2mm and 3mm wide, depending on the exact position of the fiber relative to the hydrogen flame.

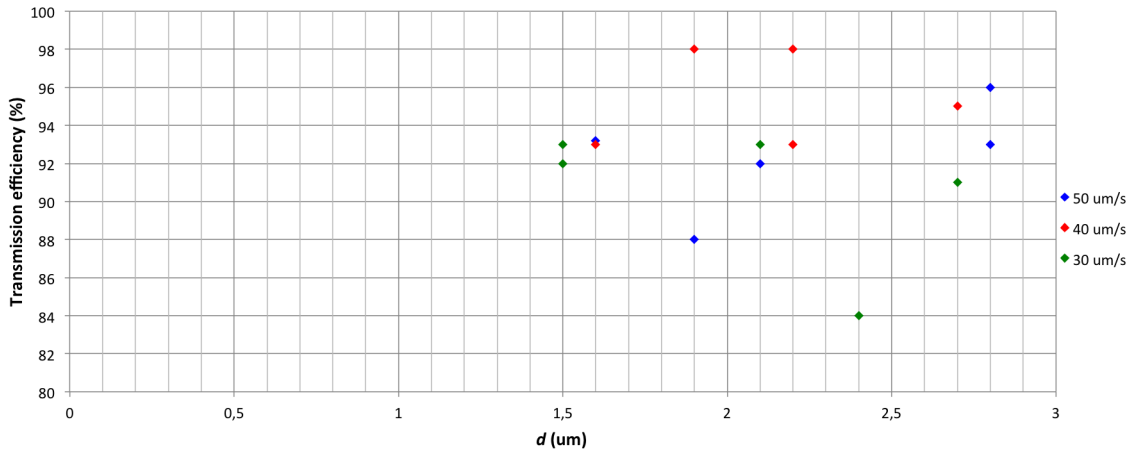


Figure 4.5: Transmission efficiency as a function of taper diameter for different pulling speeds.

The number of measurements done for each of the speeds is not enough to give a statistically significant conclusion, but from this measurements a $40\mu\text{m s}^{-1}$ pulling speed gives the highest transmission with an average of 95%. Compared with the $30\mu\text{m s}^{-1}$ and $50\mu\text{m s}^{-1}$ pulling speeds give 91% and 92% respectively. The $30\mu\text{m s}^{-1}$ give the smallest average diameter of the tapered region with $2,0\mu\text{m}$.

In figure 4.6 is the measured diameter as a function of pulling length shown. The $40\mu\text{m s}^{-1}$ pulling speed has the highest transmission, but also the longest pulling length which is in agreement with previous measurements and expectations. A pulling speed of $50\mu\text{m s}^{-1}$ give the shortest pulling length of 11mm compared to 12mm and 14mm for $30\mu\text{m s}^{-1}$ and $40\mu\text{m s}^{-1}$.

The length of the hot-zone differs from the initially expected 4 mm, which automatically gives a different pulling length (see also table B.2 in appendix B). According to equation 2.21 the theoretical pulling length is equal to 14,1 mm for a hot-zone of 3 mm and a 9,43 mm pulling length for a 2 mm hot-zone. This is more in agreement with the measurements than the initial expected 4 mm pull where the fibers should be pulled to 18,8 mm. For example, a measurement at $40\mu\text{m s}^{-1}$ with a hot-zone of 3,4 mm should in theory be stretched to 16,0 mm, but it is stopped at a distance of 14,0 mm, resulting in a diameter larger than the theoretical $1,2\mu\text{m}$ ($1,9\mu\text{m}$ measured instead).

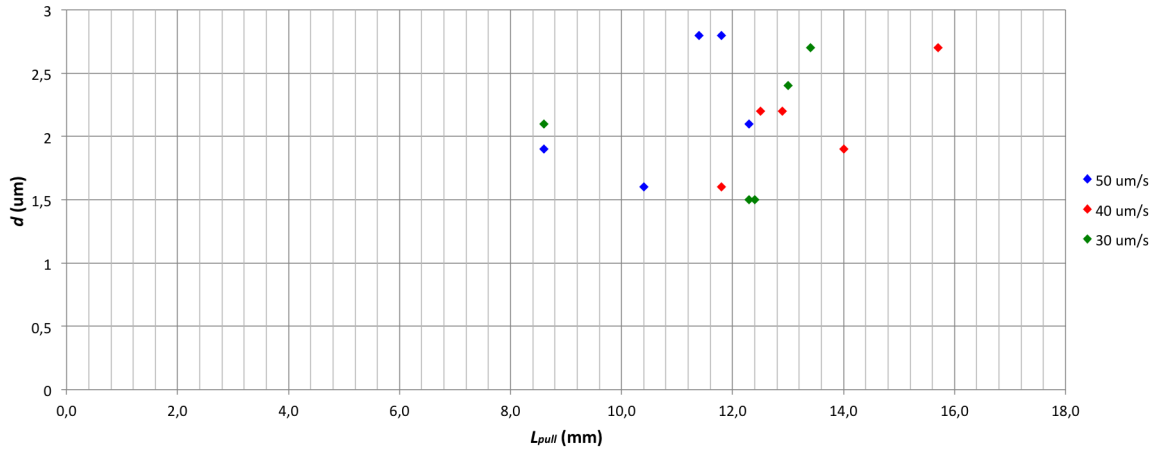


Figure 4.6: Measured diameter as a function of the pulling distance for different pulling speeds.

4.3 Error analysis

For calculating the diameter of the tapered fiber, equation 2.20 is used. This is mainly depending on three parameters, each with a certain error.

For the initial diameter of the fiber, the uncertainty is $\Delta d_0 = 0,7\mu\text{m}$. [21]. The second quantity is the pulling distance, which is determined by multiplying the driving speed with the pulling time. The driving speed has a accuracy of $\Delta v = 0,5\mu\text{m s}^{-1}$ [23]. The error in determining the pulling time differs for each measurement around a couple of seconds.

The error in the distance at a speed of $50\mu\text{m s}^{-1}$ according to equation 4.2 is $\Delta x = 0,44\text{mm}$, if $\Delta t = 5\text{s}$ and the pulling distance is chosen $18,8\text{mm}$ ($t = 376\text{s}$) as determined in chapter 3. The hot-zone is estimated to be around 4mm with an error of $\Delta L_{hz} = 0,5\text{ mm}$.

The most probable error of the tapered diameter can be determined by calculating the square root of the sum of the partial derivative of each parameter, shown in

$$\begin{aligned}\Delta d_1 &= \sqrt{\left|\frac{\delta d_1}{\delta d_0}\right|^2 \Delta d_0^2 + \left|\frac{\delta d_1}{\delta x}\right|^2 \Delta x^2 + \left|\frac{\delta d_1}{L_{hz}}\right|^2 \Delta L_{hz}^2} \\ &= \sqrt{\left|e^{\frac{-x}{L_{hz}}}\right|^2 \Delta d_0^2 + \left|-\frac{d_0 \cdot e^{\frac{-x}{L_{hz}}}}{L_{hz}}\right|^2 \Delta x^2 + \left|\frac{d_0 x \cdot e^{\frac{-x}{L_{hz}}}}{L_{hz}^2}\right|^2 \Delta L_{hz}^2}\end{aligned}\quad (4.4)$$

When the uncertainty is calculated with the given values and errors, the tapered region has a uncertainty of $\Delta d_1 = 0,69\mu\text{m}$. The estimated diameter of the fiber if pulled with this pulling length is $1,2\mu\text{m}$ which give an error of more than half of the diameter.

The biggest improvements can be made with the determination of the hot-zone. If this can be more accurately measured, the error would decrease and the taper diameter will be known with a greater accuracy.

The errors are calculated for all the measurements from figure 4.3 in table B.1 from appendix B

The errors when the diameter is calculated based on pulling distances are relatively very large. Measuring the diameters is a more reliable method of getting the diameter of the tapered region. The most probable error that is made can be estimated using equation 4.3. Using a similar approach like equation 4.4 gives

$$\begin{aligned}\Delta d_1 &= \sqrt{\left|\frac{\delta d_1}{\delta d_0}\right|^2 \Delta d_0^2 + \left|\frac{\delta d_1}{\delta l'_0}\right|^2 \Delta l_0^2 + \left|\frac{\delta d_1}{\delta l'_1}\right|^2 \Delta l_1^2} \\ &= \sqrt{\left|\frac{l'_1}{l'_0}\right|^2 \Delta d_0^2 + \left|-\frac{d_0 \cdot l'_1}{l'_0}\right|^2 \Delta l_0^2 + \left|\frac{d_0}{l'_0}\right|^2 \Delta l_1^2}\end{aligned}\quad (4.5)$$

The measured distances between the red arrows of figure 4.4 are, after taken the magnification into account, for example $l_0 = (1,8 \pm 0,025)$ mm and $l_1 = (0,03 \pm 0,005)$ mm. This gives according to the latter equation an error in the measured diameter of $\Delta d_1 = 0,35 \mu\text{m}$. This error is about half of the uncertainty based on the calculation of the diameter. The errors of the measurements are all based on this method and are given in table B.2.

5 Conclusion

To prepare an optical fiber for evanescent coupling, the fiber is tapered to increase the evanescent field outside the fiber. Subsequently the fiber is dimpled for easier use and better control of the coupling. This tapering and dimpling is done with a Corning SMF-28e+ optical fiber with a radius of $125\mu\text{m}$.

Before it can be tapered, the fiber is heated using a hydrogen flame so it becomes soft, allowing it to be stretched without damaging or breaking it. The set up is placed in an enclosure to prevent the flame from moving due to the air currents. Different speeds have been tested in the range $30\mu\text{m s}^{-1} < v < 50\mu\text{m s}^{-1}$. The fiber should not contain any damages, as this can cause the fiber to break before it becomes single mode or give a low transmission output due to scattering of the guided light. The expected diameter of the fiber after tapering is around $1,2\mu\text{m}$. The laser that is used for measuring the transmission output, was set for a wavelength of $\lambda = 1550\text{nm}$.

With the measured pulling length of the fiber when it becomes single mode and an estimation of the hot-zone length, the diameter of the fiber can be calculated. This is, depending on the pulling length, fluctuating between $3\mu\text{m}$ and the $15\mu\text{m}$. The pulling length changes between different measurements from $8,5\text{ mm}$ up to $16,5\text{ mm}$. Distances higher than 12 mm give the highest transmission efficiency with an average of 85% . Shorter pulling lengths result in an average efficiency of 70% for all the speeds. The reason for the relative large difference between the pullings is because the equation is depending on the hot-zone which is not known with a great accuracy. The uncertainty in the initial diameter of the fiber and the error in the pulling length are relative small, so the error is mainly depending on the uncertainty in the hot-zone length. Because the diameter of the fiber is depending on the hot-zone according to an exponential function, the errors are large with a maximum error up to $4,0\ \mu\text{m}$.

The frequency of the oscillations is not increasing at higher pulling speeds. This is because the doping concentration is not immediately equally distributed in the fiber after the core and the cladding melt together.

With the use of a microscope with a maximum of $100\times$ magnification, the diameter of the fiber can be measured instead of being calculated. This can be done without knowing the hot-zone length what results in a more reliable measuring of the tapered region diameter. The diameter is showed to be more constant when it is measured, with a diameter between $2\mu\text{m}$ and $2,5\mu\text{m}$ on average. This is about a micron larger than the expected diameter. The differences between the several measurements and the calculated value are probably because of the fact that the pulling is not always stopped right after the fiber becomes single mode or that the pulling is stopped too soon. So, most of the fibers are getting pulled a little longer or shorter, resulting in a smaller or bigger diameter of the fiber. It is not always clear when the oscillations stop, because a small misalignment can cause the signal to fluctuate, even when there is only one mode present in the fiber.

The fluctuations and the multimode oscillations can be hard to distinguished from each other. The biggest improvements can be made with aligning the fiber properly before it is heated. Also, the hydrogen flame should get placed accurately, creating a large single hot-zone. A long hot-zone causes large transition regions so that the light is very gradually guided to the thin part of the fiber. This proved to be an important factor during the experiments.

Further research

The research done so far is mainly focussed on getting tapered fibers with a constant and high transmission. This is only the first part of a bigger setup. The next important step to control is the bending and dimpling part of the setup. With the bending device is should be possible to get the tapered fiber off from the tapering setup in one piece, although presumably this would take practice. To get the fibers off for measuring the diameter under the microscope it turned out that this could be quite tricky as the fiber is really fragile. Once the fiber is placed on the bending device, the bending itself is not expected to be very difficult. Dimpling the fiber is a matter of experimenting with the several different parameters of the setup, like the flame position and height and the size of the dimple.

References

- [1] *Moore's law*. [online] Available at: <http://www.moorelaw.org> [Accessed 3 Mar. 2015].
- [2] C.V. RAMAN & G.A. SUTHERLAND, "Whispering-Gallery Phenomena at St. Paul's Cathedral". *Nature* **108**, p42. September 1921.
- [3] Photonics Integrated Circuits for Visible Light and Near Infrared. (2014). *Photonics Magazine*, 38, pp.16-18.
- [4] ASPICs: Application Specific Photonic Integrated Circuits. (2014). *Photonics Magazine*, 39, pp.5-9.
- [5] Lumerical.com, (2015). *Lumerical Solutions*. [online] Available at: https://www.lumerical.com/support/whitepaper/interconnect_ring_modulator_model.html [Accessed 29 Mar. 2015].
- [6] Hauer, B., Kim, P., Doolin, C., MacDonald, A., Ramp, H. and Davis, J. (2014). On-chip cavity optomechanical coupling. *EPJ Techniques and Instrumentation*, 1(1).
- [7] Ogawa, Y. (2011). Method of fabricating high transmission optical tapered fiber. *Tanabe Photonic Structure Group, Keio University*, 1(1).
- [8] Hecht, E. (2002). *Optics*. 4th ed. Reading, Mass.: Addison-Wesley, pp.193-199.
- [9] Hecht, E. (2002). *Optics*. 4th ed. Reading, Mass.: Addison-Wesley, pp.111-118.
- [10] Paschotta, D. (2015). *Numerical Aperture*. [online] Rp-photonics.com. Available at: http://www.rp-photonics.com/numerical_aperture.html [Accessed 5 Mar. 2015].
- [11] Kasap, S. and Sinha, R. (2013). *Optoelectronics and photonics : principles and practices*. Harlow, Essex: Pearson Education, p.47.
- [12] Kasap, S. and Sinha, R. (2013). *Optoelectronics and photonics : principles and practices*. Harlow, Essex: Pearson Education, p.116.
- [13] Kasap, S. and Sinha, R. (2013). *Optoelectronics and photonics : principles and practices*. Harlow, Essex: Pearson Education, pp.123, 131.
- [14] Pedrotti, F., Pedrotti, L. and Pedrotti, L. (1987). *Introduction to optics*. Upper Saddle River, N.J.: Prentice-Hall, p.248.
- [15] Pedrotti, F., Pedrotti, and Pedrotti, L. (1987). *Introduction to optics*. Englewood Cliffs, N.J.: Prentice-Hall, pp.504,505.
- [16] Hecht, E. (2002). *Optics*. 4th ed. Reading, Mass.: Addison-Wesley, pp.124-126.
- [17] Ding, L., Belacel, C., Ducci, S., Leo, G. and Favero, I. (2010). Ultralow loss single-mode silica tapers manufactured by a microheater. *Applied Optics*, 49(13), p.2441.

- [18] Imedeia.uib-csic.es, (2015). *Understanding Optical Communications:Optical Fibre*. [online] Available at: http://imedeia.uib-csic.es/salvador/coms_optiques/addicional/ibm/ch02/02-09.html Heading15 [Accessed 7 Mar. 2015].
- [19] IBM Redbooks. (1998). *Understanding Optical Communications*. IBM Corporation.
- [20] MIT, (2005). *Gauss Law*. [online] Available at: <http://web.mit.edu/8.02T/www/802TEAL3D/visualizations/coursenotes/modules/> [Accessed 27 Mar. 2015].
- [21] Corning.com, (2015). *SMF28 Ultra fiber*. [online] Available at: http://www.corning.com/opticalfiber/products/ultra_fiber.aspx [Accessed 03 Apr. 2015].
- [22] http://www.engineeringtoolbox.com/flame-temperatures-gases-d_422.html, (2015). *Flame temperatures some common gases*. [online] Available at: http://www.engineeringtoolbox.com/flame-temperatures-gases-d_422.html [Accessed 03 Apr. 2015].
- [23] Eng.surugaseiki.com, (2015). *SURUGA SEIKI CO., LTD.*. [online] Available at: <http://eng.surugaseiki.com/index.php?n=050200502> [Accessed 9 Apr. 2015].
- [24] Birks, T. and Li, Y. (1992). The shape of fiber tapers. *J. Lightwave Technol.*, 10(4), pp.432-438.
- [25] Siemon.com, (2015). '*Light It Up - Fiber Transmissions And Applications - Siemon Network Cabling Solutions*'. N.p.. [online]. Available at: http://www.siemon.com/us/white_papers/08-03-03-light-it-up.asp [Accessed 20 Apr. 2015].
- [26] Law.cornell.edu, (2015). *7 CFR 1755.200 - RUS standard for splicing copper and fiber optic cables. — LII / Legal Information Institute*. [online] Available at: <https://www.law.cornell.edu/cfr/text/7/1755.200> [Accessed 19 Apr. 2015].
- [27] Hoffman, J., Ravets, S., Grover, J., Solano, P., Kordell, P., Wong-Campos, J., Orozco, L. and Rolston, S. (2014). Ultrahigh transmission optical nanofibers. *AIP Advances*, 4(6), p.067124.
- [28] Paschotta, D. (2015). *Encyclopedia of Laser Physics and Technology - Faraday isolators, circulators, optical isolators*. [online] Rp-photonics.com. Available at: http://www.rp-photonics.com/faraday_isolators.html [Accessed 2 May 2015].

A Supplementary information chapter 3

In chapter 3, a method is described how the diameter of a fiber can be calculated as a function of speed and time. This equation arises from the law of conservation of mass. It is presumed that during heating the mass of the fiber remains constant, and so does the volume. This can be seen in

$$m = \rho V \quad (\text{A.1})$$

Where ρ [kg m^{-3}] is the density of the medium. If the mass and the density of the medium remain the same, the volume should also be constant. The fiber can be interpreted as a cylinder with an initial radius r_0 [m] and a length L_0 [m], where the volume V_0 [m^3] is

$$V_0 = \pi r_0^2 L_0 \quad (\text{A.2})$$

As the fiber is pulled to length $(L_0 + \delta L)$, the radius of the fiber waist decreases to $(r_0 - \delta r)$. So the volume V_1 [m^3] becomes

$$V_1 = \pi (r_0 - \delta r)^2 \cdot (L_0 + \delta L) \quad (\text{A.3})$$

The volume should still remain constant, so

$$V_0 = V_1 \quad (\text{A.4})$$

$$r_0^2 L_0 = (r_0 - \delta r)^2 \cdot (L_0 + \delta L) \quad (\text{A.5})$$

The hot-zone L_{hz} is ideally the only part that is getting thinner during pulling. After a pulling distance L_{pull} the diameter of the hot zone is decreased to a diameter $(r - \delta r)$.

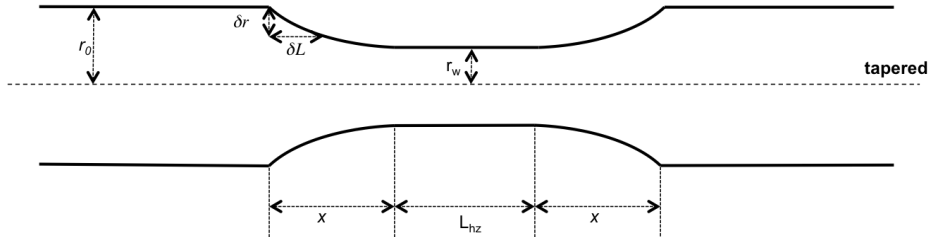


Figure A.1: Schematic representation of a tapered fiber with the quantities that are used in this appendix.

For a small time interval ($\delta t \rightarrow 0$) this can be transformed in a differential equation

$$\frac{dr}{dL_{pull}} = -\frac{r}{2L_{hz}} \quad (\text{A.6})$$

$$\frac{dr}{r} = -\frac{dL_{pull}}{2L_{hz}}$$

The fiber is getting equally pulled from both sides, so the transition region x is the same on both sides. The length of the taper region, considering that the hot-zone remains constant during stretching, can be written as

$$\begin{aligned} L_{pull} + L_{hz} &= L_{hz} + 2x \\ L_{pull} &= 2x \end{aligned} \quad (\text{A.7})$$

The differential equation can be solved with a definite integral from the initial radius r_0 to the taper radius r_w . This is equal to the definite integral of a pulling distance L_{pull} in the range of $0 < L_{pull} < 2x$

$$\int_{r_0}^{r_w} \frac{1}{r} dr = \int_0^{2x} -\frac{1}{2L_{hz}} dL_{pull} \quad (\text{A.8})$$

This can be solved as

$$[\ln(r)]_{r_0}^{r_w} = -\frac{2x}{2L_{hz}} \quad (\text{A.9})$$

$$\ln(r_w) - \ln(r_0) = \ln\left(\frac{r_w}{r_0}\right) = -\frac{x}{L_{hz}}$$

To solve this for the final fiber radius, it becomes

$$\begin{aligned} \frac{r_w}{r_0} &= e^{-\left(\frac{x}{L_{hz}}\right)} \\ r_w &= r_0 e^{-\left(\frac{x}{L_{hz}}\right)} \end{aligned} \quad (\text{A.10})$$

It should be noted that this equation is only true for a constant hot-zone. [24]

B Tables

This appendix shows a overview of measurements that has been done. The acceleration time and the delay time are constant at 500ms and 5s respectively. In table B.1 the diameter of the hot-zone and the error in this diameter are calculated based on the measured values. The hot-zone is estimated to extend over $4,0\pm 0,5\text{mm}$. The pulling distance is calculated by multiplying the speed of the stages to the time until the fiber becomes single mode again minus the delay time as seen in equation 4.1. The error in the diameter is determined with equation 4.4. The error in the pulling length that is needed for calculating this error is determined with equation 4.2.

Table B.1: Table with tapering results. Shown are respectively the driving speed, time where the fiber is single mode until it becomes multimode ('sm' subscript), time where the fiber is multimode until it becomes single mode again ('mm' subscript), pulling length, new diameter of the tapered region (calculated based on the pulling length), the error in the new diameter and the transmission efficiency of the fiber relative to the initial transmission of the laser light.

v [$\mu\text{m s}^{-1}$]	t_{sm} [s]	t_{mm} [s]	l_{pull} [mm]	d_1 [μm]	Δd_1 [μm]	η [%]
30	97	485	14,4	3,5	1,6	86
30	84	445	13,2	4,7	1,9	85
30	89	352	10,4	9,4	3,1	61
30	102	370	10,9	8,3	2,8	75
30	98	425	12,6	5,5	2,1	78
30	100	434	12,9	5,1	2,1	68
30	73	413	12,2	5,9	2,3	90
40	65	220	8,6	14,9	4,0	63
40	140	400	15,8	2,5	1,2	93
40	65	250	9,8	11,0	3,4	78
40	132	290	11,4	7,4	2,6	71
40	130	288	11,3	7,6	2,7	71
40	62	355	14,0	3,7	1,7	62
40	59	238	9,3	12,5	3,7	68
40	61	268	10,5	9,2	3,0	81
40	75	415	16,4	2,1	1,0	93
50	52	215	10,5	9,2	3,1	69
50	60	261	12,8	5,2	2,1	83
50	45	188	9,2	13,9	3,7	56
50	25	203	9,9	10,8	3,5	69
50	67	211	10,3	9,7	3,2	84
50	50	250	12,3	5,9	2,3	96

In table B.2 the results from the new calibrated setup is shown. The diameter of the fiber is measured with the microscope as explained in chapter 4.2. With this diameter and the pulling length of the fiber, the length of the hot-zone is calculated with equation 2.20.

Table B.2: Table with tapering results from the new calibrated setup. Shown are respectively the driving speed, time where the fiber is single mode until it becomes multi mode, time where the fiber is multi mode until it becomes single mode again, pulling length, new diameter of the tapered region, the error in the new diameter, the calculated hot-zone based on the measured diameter and the transmission efficiency of the fiber relative to the initial transmission of the laser light.

v [$\mu\text{m s}^{-1}$]	t_{sm} [s]	t_{mm} [s]	l_{pull} [mm]	d_1 [μm]	Δd_1 [μm]	L_{hz} [mm]	η [%]
30	95	450	13,4	2,7	0,36	3,5	91
30	94	445	13,2	2,4	0,37	3,3	84
30	81	400	11,9	2,1	0,40	2,1	93
30	90	416	12,3	1,5	0,35	2,8	92
30	92	418	12,4	1,5	0,30	2,8	93
40	68	318	12,5	2,2	0,34	3,1	93
40	60	396	15,6	2,7	0,27	4,1	95
40	30	331	13,0	2,2	0,36	3,2	98
40	64	299	11,8	1,6	0,37	2,7	93
40	66	355	14,0	1,9	0,34	3,4	98
50	55	240	11,8	2,8	0,25	3,1	96
50	50	250	12,3	2,1	0,35	3,0	92
50	50	235	11,5	2,8	0,33	3,0	93
50	47	210	10,3	1,6	0,41	2,4	93
50	45	171	8,3	1,9	0,39	2,0	88

open Bachelor / Master position

Department of Quantum Nanoscience
Delft University of Technology

Type of position: 3 - 9 month project for Bachelor or Master program. The depth and focus can be adjusted to fit the length of the particular project and personal preference of the student.

Supervisor: Dr. Simon Gröblacher

Project title: High-efficiency coupling of light to an on-chip optomechanics device

Project description: In the field of optomechanics light is coupled to mechanical motion via the radiation-pressure force, with the goal of observing macroscopic quantum behavior of mechanical systems. For this to become feasible, the read-out mechanism of any quantum state has to be highly efficient in order to avoid mixing it with noise. In the *Groebblacher lab* we use a laser field to measure the mechanical degree of freedom of, for example, a GHz phononic structure made of Silicon. The coupling is achieved through a fiber taper and an optical waveguide on the chip, which can in principle achieve efficiencies in excess of 95%. The envisioned project includes fabrication of high-quality fiber tapers and the design of waveguides on a Silicon wafer, coupled to photonic crystal cavities. In addition, the project will include the development and testing of such a high-efficiency coupling method at cryogenic temperatures.

The Department of Quantum Nanoscience at the TU Delft is an exciting, collaborative environment with several world-renowned research groups. The department is focused on Quantum Theory, Quantum Information Science and Quantum Devices & Materials. The research is supported by state-of-the-art facilities, in particular the cleanroom facilities for realizing next-generation nanostructures.

The successful candidate will have the opportunity to learn new experimental techniques (fiber taper pulling, optical testing, cryogenics, ...), understand the underlying principles of optomechanical systems (classical / quantum mechanics, condensed matter physics, optics) and to gain a basic knowledge in finite element simulation and advanced computer based experimentation (IPython, Matlab, C#, ...).

Additional information: <http://groebblacherlab.tudelft.nl>

Contact: Please send inquiries / applications (cover letter, CV, reference letters) to s.groebblacher@tudelft.nl.